Quantum-mechanical analogy of beam propagation in waveguides with a bent axis: Dynamic-mode stabilization and radiation-loss suppression

S. Longhi, D. Janner, M. Marano, and P. Laporta

Istituto Nazionale per la Fisica della Materia, Dipartimento di Fisica, Politecnico di Milano, Piazza L. da Vinci 32, I-20133 Milan, Italy

Wave propagation in an optical waveguide with a bent axis is studied under the scalar and paraxial wave approximations, and the quantum mechanical analogy with the electron dynamics in an atomic potential interacting with an intense electromagnetic field is highlighted. In particular we show that for a truncated parabolic waveguide with a periodically curved axis, a dynamic mode splitting with reduced radiation losses can be observed, which is fully analogous to the phenomenon of wave packet dichotomy and ionization quenching found in strong-field atomic physics.

I. INTRODUCTION

Wave optics and quantum mechanics, and their respective classical limits of geometric optics and Newtonian mechanics, share many similarities that are described in many introductory textbooks and reviews (see, for instance, Refs. [1,2], and references therein). This analogy has led to many relevant developments in apparently unrelated research fields; theoretical and experimental concepts and methods known in one area, in fact, have been successfully applied to the other one [2]. For instance, electromagnetic wave propagation at microwaves or at optical wavelengths has been often considered as an experimental verifiable model for many quantum-mechanical effects including, among others, the issue of tunneling times across a potential barrier [3–5], quantum chaos studies [6], and Bloch oscillations in a periodic potential [7–9]. The similarity between the Schrödinger equation for a nonrelativistic particle and the paraxial wave equation for beam propagation in dielectric structures has been widely recognized and the use of quantum mechanics in the modeling of waveguides and multimode optical fibers has been pursued by many authors [10–20]. In particular, it has been shown that the operator formalism of quantum mechanics provides elegant solutions for problems associated with beam propagation in graded-index multimode slab waveguides and fibers [13,15,17,19,20]; mode coupling and waveguide losses in coupled or bent waveguides have been studied as well in the framework of the scattering theory of quantum mechanics in Refs. [14,21]. More recently, many concepts and methods of solid-state physics have been successfully employed in the study of photonic band gap structures and devices (see, for instance, [22,23]).

The aim of this paper is to point out a rather general and elegant analogy between paraxial beam propagation in an optical waveguide with a bent axis and electron dynamics in an atomic system interacting with an electromagnetic field. This analogy stems from the formal equivalence of the scalar and paraxial beam propagation equation for the waveguide and the one-electron time-dependent Schrödinger equation with an electromagnetic interaction term written in the Kramers-Henneberger reference frame [24–26]. Following this analogy, we study in detail the case of a waveguide with a sinusoidally curved axis, corresponding to a monochromatic electromagnetic field in the quantum-mechanical case. We show that many unexpected effects found in high-intensity, high-frequency atom-field interactions, such as reduction of the ionization rate due to adiabatic stabilization and wave packet dichotomy [26–32], may be observed in such waveguides. Our optical model bears as well a close connection with the wave packet dynamics of Bose-Einstein condensates in a periodically shaken trap, recently studied in Ref. [33].

The paper is organized as follows. In Sec. II, the waveguide model is briefly reviewed and the quantum-mechanical analogy is outlined. In Sec. III, beam propagation in a periodically curved waveguide with a truncated parabolic index profile is considered, and the effects of loss reduction and dynamic wave packet splitting, analogous to the quantum-mechanical effects encountered in atomic physics with super-intense laser fields [26], are analytically and numerically studied. Finally, in Sec. IV, the main conclusions are outlined.

II. THE OPTICAL-MECHANICAL ANALOGY: WAVE PROPAGATION IN A WAVEGUIDE WITH A DISTORTED OPTICAL AXIS AND THE KRAMERS-HENNEBERGER SCHRÖDINGER EQUATION

The starting point of our analysis is provided by the scalar wave equation for beam propagation in a weakly guiding dielectric waveguide in the paraxial approximation. The guide axis is allowed to weakly and slowly deviate from straightness, and we indicate by $x=x_0(z)$ and $y=y_0(z)$ the Cartesian equations of the curved axis, where z is the direction of the straight waveguide and (x,y) are the transverse coordinates [see Fig. 1(a)]. In this case, the paraxial wave equation describing the propagation of a monochromatic scalar field $\psi(x,y,z)$ with a vacuum wave number k_0 reads (see, for instance, Refs. [34–36])

$$\frac{\partial \psi}{\partial z} = \frac{i}{2k_0 n_0} \nabla^2_{x,y} \psi + i \frac{k_0}{2n_0} \{n^2[x-x_0(z), y-y_0(z)] - n_0^2\} \psi,$$
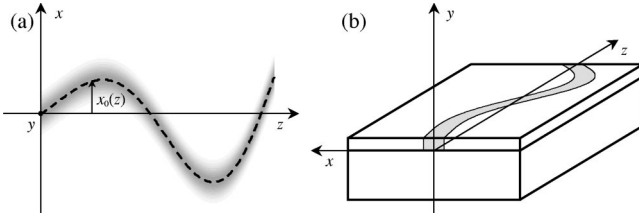
$$(1)$$

FIG. 1. (a) Schematic of a weak waveguide with a distorted optical axis. The direction z in the figure is the paraxial axis of the corresponding straight waveguide, $x_0(z)$ and $y_0(z)$ are the equations of the curved axis, and the shaded area is the high-index waveguiding region. (b) Schematic of a weak channel waveguide with a distorted optical axis written onto a strongly confining planar waveguide. The weak guiding of the channel structure is provided by a graded-index profile in the x direction, whereas the tight confinement in the y direction is achieved by a high-contrast steplike refractive index profile of the planar structure.

where $n(x,y)$ is the transverse refractive index profile of the straight waveguide, n_0 is the cladding layer index, and $\nabla^2_{x,y} \equiv \partial^2/\partial x^2 + \partial^2/\partial y^2$ is the transverse Laplacian. The scalar and paraxial wave equation provides an appropriate model for the full vectorial Maxwell equations, provided that the refractive index contrast of the guide is weak ($|n(x,y,z) - n_0| \ll n_0$), the diffractive length of the fundamental guided mode is much larger than the wavelength $\lambda_0 = 2\pi/k_0$, and the refractive index $n(x,y,z)$ varies slowly with respect to the paraxial direction z, over one wavelength λ_0 ($\lambda_0|\partial n/\partial z| \ll n_0$). We note that, in case of a straight waveguide with a parabolic-index profile, Eq. (1) has been widely adopted as a model for graded-index parabolic waveguides and lenses, and the analogy of such an equation with the time-dependent Schrödinger equation for a two-dimensional harmonic oscillator has been discussed in many papers (see, for instance, Ref. [19]). Here we would like to show rather generally that, in presence of waveguide axis distortions, the quantum-mechanical analog of Eq. (1) is the time-dependent Schrödinger equation for a charged particle in a two-dimensional potential interacting with an electromagnetic field, the potential vector **A** associated with the electromagnetic field being related to the waveguide axis distortion through a simple relation [see Eq. (6) below]. In fact, let us consider the time-dependent Schrödinger equation for a charged particle, of charge q and mass m (e.g., an electron), in a two-dimensional potential $V(X,Y)$ (e.g., the atomic binding potential), interacting with an electromagnetic field derived from the vectorial potential $\mathbf{A}(t) = A_x\mathbf{u}_x + A_y\mathbf{u}_y$. Assuming the Lorentz gauge, the equation for the particle wave function $\phi(X,Y,t)$ reads

$$i\hbar \frac{\partial \phi}{\partial t} = -\frac{\hbar^2}{2m}\nabla^2_{X,Y}\phi + \frac{q^2 A^2}{2m}\phi$$

$$-i\hbar\frac{q}{m}\left(A_x\frac{\partial}{\partial X} + A_y\frac{\partial}{\partial Y}\right)\phi + V(X,Y)\phi. \quad (2)$$

To show the formal equivalence of Eqs. (1) and (2), it is worth to rewrite Eq. (2) by introducing the Kramers-Henneberger (KH) transformation, which is commonly adopted in atomic physics to study the interaction of a bound electron with superhigh intensity and high-frequency laser fields [24–26]. The KH transformation basically corresponds to a change of the reference frame from the atomic rest frame to the moving coordinate frame of the completely free charged particle responding to the applied electromagnetic field [see Eq. (4) below]. Let us introduce the phase transformation

$$\phi = \psi \exp\left[-i\frac{q^2}{2m\hbar}\int^t dt' A^2(t')\right], \quad (3)$$

and the change of variables

$$x = X - \frac{q}{m}\int^t dt' A_x(t'), \quad y = Y - \frac{q}{m}\int^t dt' A_y(t'). \quad (4)$$

Then Eq. (2) takes the form of the Kramers-Henneberger Schrödinger equation,

$$i\hbar\frac{\partial\psi}{\partial t} = -\frac{\hbar^2}{2m}\nabla^2_{x,y}\psi + V[x - x_0(t), y - y_0(t)]\psi, \quad (5)$$

where $x_0(t)$ and $y_0(t)$ describe the classical (nonrelativistic) trajectory of the charged particle, in absence of the binding potential, interacting with the electromagnetic field solely, that is,

$$x_0(t) = -\frac{q}{m}\int^t dt' A_x(t'), \quad y_0(t) = -\frac{q}{m}\int^t dt' A_y(t'). \quad (6)$$

A comparison of Eqs. (1) and (5) reveals the formal analogy of the two equations. Indeed, Eq. (1) can be interpreted as the Kramers-Henneberger Schrödinger equation for a particle of mass $m = n_0$ in a potential $V(x,y) = [n_0^2 - n^2(x,y)]/(2n_0) \simeq n_0 - n(x,y)$ with the formal substitution $\lambda_0 = h$ for the wavelength and $z = t$ for the paraxial coordinate. The equations for the tilted waveguide axis, $x_0(z)$ and $y_0(z)$, are just the trajectories of the free particle as given in Eq. (6).

The presented analogy allows one to capture the effects of waveguide axis distortions on beam propagation in terms of stimulated transitions among the modes of the straight waveguide (either bound or unbound modes) in the same way as in the atomic case, where the applied field produces transitions among the electronic energy states, including those to unbounded states (ionization). Radiation losses in the waveguide due to axis distortions are thus analogous to the process of ionization of the atom and are ruled by the same laws of quantum mechanics. In particular, of major relevance in the framework of this analogy is the case of a waveguide with a *periodically* curved axis, which corresponds to the interaction with a monochromatic field in the atomic case. Such a case will be considered in detail in the following section, where the optical analog of many anomalous effects found in high-field atomic physics, such as quenching of ionization rate and dynamic wave packet splitting, will be retrieved. In the following, we will be mainly concerned with a one-dimensional waveguide scheme [36], corresponding to a one-dimensional KH Schrödinger equation in the quantum-

mechanical analogy. Such a case corresponds, for instance, to a weak channel waveguide with a distorted axis realized on a planar waveguide, which provides a tight field confinement in one transverse direction, e.g., in the y direction, as shown in Fig. 1(b) (see, e.g., Ref. [37]). In this case, by assuming a refractive index profile $n(x,y,z)=n_0(y)$ $+\Delta n(x,y,z)$, where $n_0(y)$ is the steplike profile of the tightly confining planar waveguide and $\Delta n(x,y,z)$ provides the weak guiding of the superimposed channel waveguide ($|\Delta n| \ll n_0$), one can derive, using multiple-scale analysis or effective-index methods, an effective one-dimensional propagation equation for the field envelope in the weakly guided transverse x direction after eliminating from Eq. (1) the y dependence of the field provided by the tightly confining planar structure. In the spirit of the weak guiding approximation, one can also set $n^2-n_0^2 \simeq 2n_0(n-n_0)$, so that the one-dimensional paraxial beam propagation equation in the waveguide reads

$$\frac{\partial \psi}{\partial z} = \frac{i}{2k_0 n_0} \frac{\partial^2 \psi}{\partial x^2} + ik_0\{n[x-x_0(z)]-n_0\}\psi. \qquad (7)$$

III. FIELD PROPAGATION IN A PERIODICALLY CURVED WAVEGUIDE: DYNAMIC MODE SPLITTING AND RADIATION MODE REDUCTION

A case of major relevance within the framework of the quantum-mechanical analogy considered in Sec. II is that of a sinusoidally curved waveguide, for which $x_0(z)$ $=A(z)\cos(2\pi z/\Lambda)$, where A is the modulation depth and Λ the spatial period of the modulation. This case is analogous to the interaction of a bound electron with a monochromatic field. In general, we will allow the modulation amplitude A to vary slowly with z, as compared to the spatial modulation period Λ, in order to study the coupling from, e.g., a straight waveguide into a periodically curved one. The quantum-mechanical analog is the interaction of a bound electron with, e.g., a nearly monochromatic light laser pulse, for which the issue of pulse adiabaticity is of major importance in the onset of wave packet localization and ionization suppression (see, e.g., Ref. [30]). As an index profile $n=n(x)$ for the straight waveguide, we will consider specifically the truncated parabolic graded-index profile, i.e.,

$$n(x) = \begin{cases} n_0 & \text{for} \quad |x|>a \\ n_0+\Delta n_0\left(1-\dfrac{x^2}{a^2}\right) & \text{for} \quad |x|<a, \end{cases} \qquad (8)$$

where $2a$ is the width of the waveguide, n_0 is the bulk refractive index, and $n_0+\Delta n_0$ is the on-axis refractive index. We note that the case of a periodically curved graded-index waveguide with a nontruncated parabolic-index profile corresponds to the quantum dynamics of a harmonic oscillator with an external sinusoidal driving force, which has been widely investigated in the literature (see, for instance, Ref. [38], and references therein). The optical analog was also previously studied using either a Green function approach [21] or a generalized *ABCD* matrix formalism commonly adopted in paraxial Gaussian beam optics [39]. In this case, a wave packet spreading has been predicted for a modulation period Λ equal to the characteristic spatial period of the lens guide (see Ref. [39]), which corresponds in the geometric optics limit to the secular growth of ray oscillations around the undistorted waveguide axis due to the resonant excitation of the classical harmonic oscillator. The case of a truncated parabolic-index slab waveguide with a bent axis was considered by Marcuse [40] assuming a *weak axis deformation*, and an approximate analytical expression for the power radiation loss induced by a periodic modulation of the waveguide axis was derived in a perturbative manner which resembles the above-threshold ionization rate calculation in the Keldysh theory of multiphoton ionization (see, for instance, Sec. 3.2 in Ref. [26]). In such a theory, radiation losses during beam propagation are due to the coupling of the fundamental confined mode of the waveguide with radiation (unbounded) modes of the straight waveguide induced by the periodic axis bending, and the radiation-loss rate turns out to increase as the depth of bending is increased. In the present work, removing the weak axis deformation approximation, we show that the qualitative behavior of wave propagation is substantially different from those predicted by the first-order perturbative analysis [40], especially when considering short spatial modulations and amplitude A of waveguide distortion comparable with (or larger than) the waveguide width $2a$. In such a situation, a completely different and rather unusual scenario sets in, namely, the occurrence of a dynamic-mode stabilization, which manifests itself by a mode splitting during the propagation, and the corresponding reduction of radiation losses. Owing to the analogy of the paraxial beam propagation equation with the Kramers-Henneberger Schrödinger equation, such phenomena provide in the optical context an experimentally verifiable framework of electron dynamic wave stabilization, ionization suppression, and wave packet dichotomy found in high-field atomic physics [26].

A. Dynamic-mode splitting and the average waveguide model

We have studied the beam propagation in the truncated parabolic-index waveguide with a periodically curved axis by direct numerical simulations of the paraxial wave equation (7) using either a pseudospectral split-step method or a finite difference Crank-Nicolson method with absorbing boundary conditions (see, e.g., Ref. [36]). In a first set of simulations, we launched into the waveguide the Gaussian-like mode supported by the straight waveguide and we increased adiabatically the modulation depth A using a quarter-wave sine-square law, i.e., we assumed $A(z)$ $=A_0\sin^2[\pi z/(2L_a)]$ for $0<z<L_a$ and $A=A_0$ for $z>L_a$, where $L_a \gg \Lambda$ is the length of the adiabatic section of the waveguide. The beam propagation after the adiabatic section turns out to strongly depend on the final modulation depth A_0 and on the spatial modulation period Λ. For long modulation periods, the beam shape remains almost Gaussian and follows adiabatically the trajectory of the curved waveguide axis, though high radiation losses appear due to the periodic axis bending (see Fig. 2). Conversely, a beam splitting is observed when the modulation period is short enough as
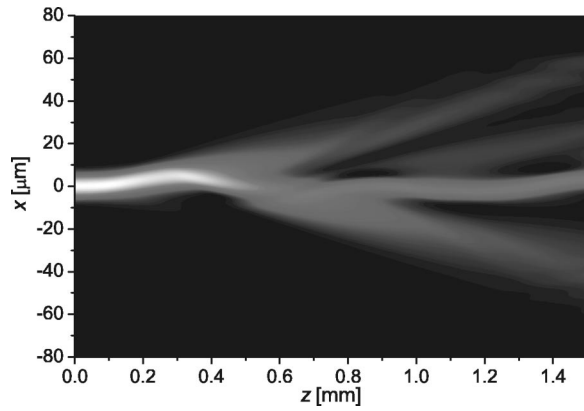
FIG. 2. Beam propagation in a truncated parabolic waveguide with a slowly modulated periodic axis bending. Parameter values are $n_0 = 1.538$, $a = 8$ μm, $\Delta n_0 = 0.01$, $\lambda_0 = 1.55$ μm, $A_0/a = 0.5$, and $\Lambda = 600$ μm.

compared to the diffractive length of the mode in the straight waveguide, provided that the modulation depth is comparable with or larger than the waveguide width. The beam splitting observed after the adiabatic section is analogous to the wave packet dichotomy found in the quantum-mechanical context [26,29]. An example of transition from the lossy mode propagation regime (Fig. 2) to the stabilization mode and dynamic-mode splitting regimes, observed at short modulation periods, is shown in Figs. 3 and 4 for increasing values of the modulation depth A_0; parameter values chosen in Figs. 2–4 are $\lambda_0 = 1.55$ μm, $a = 8$ μm, $n_0 = 1.538$, and $\Delta n_0 = 0.01$. As the modulation depth is increased, a transition from a mode broadening regime (Fig. 3) to a mode splitting regime (Fig. 4) is observed. A detailed evolution of the beam intensity profile during propagation in the mode splitting regime is reported in Fig. 5. Note that the two lobes of the splitted beam turn out to be symmetrically
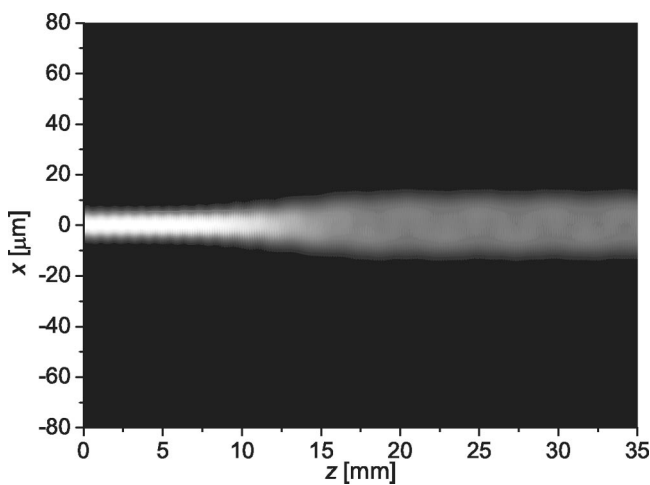

FIG. 3. Beam propagation in a truncated parabolic waveguide with a short modulation period. The waveguide is composed by an adiabatic zone ($0 < z < 20$ mm), where the axis modulation depth slowly increases with a sine-square law, followed by a uniformly-periodic region (20 mm $< z < 35$ mm). Parameter values are the same as in Fig. 2, except for $\Lambda = 157$ μm and $A_0/a = 0.875$.
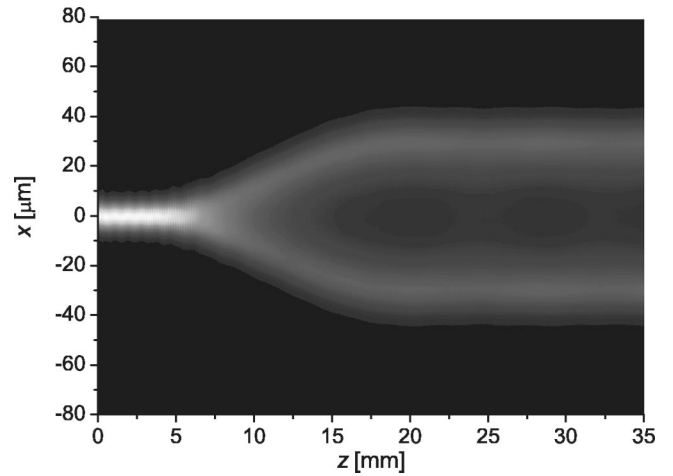

FIG. 4. Beam propagation in a truncated parabolic waveguide in the dynamic beam splitting regime. The waveguide structure is the same as in Fig. 3. Parameter values are as in Fig. 3, except for $A_0/a = 4.375$.

localized at distances of $\simeq \pm A_0$ from the straight z axis. The main physical reason underlying the occurrence of the dynamic-mode splitting is that, for a periodic modulation Λ shorter than the diffractive length of the fundamental straight waveguide mode, the beam propagation along the waveguide as described by Eq. (7) corresponds, at leading order, to the propagation in a *straight* waveguide with an effective refractive index profile $n_{av}(x,z)$ which is obtained by averaging, with respect to the propagation spatial variable z over one modulation period, the actual refractive index profile $n[x - x_0(z)]$, i.e.,

$$n_{av}(x,z) = \frac{1}{\Lambda} \int_0^\Lambda n[x - A\cos(2\pi z/\Lambda)]dz$$

$$= \frac{1}{\pi} \int_{-1}^1 \frac{n(x - Au)}{\sqrt{1 - u^2}} du, \quad (9)$$

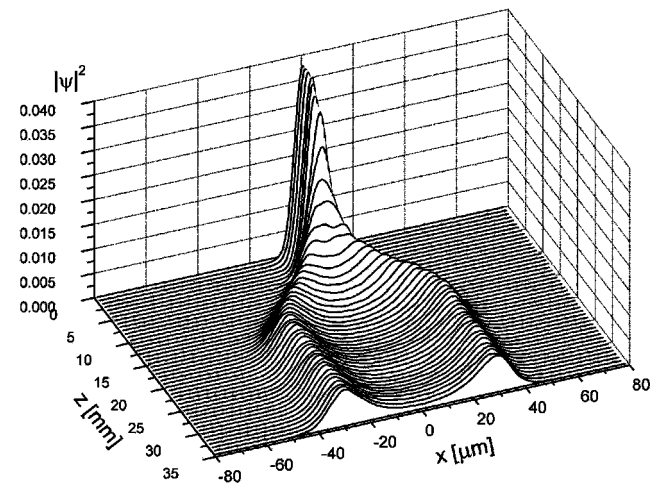where the dependence of n_{av} on z comes from the possible

FIG. 5. Evolution of beam intensity $|\psi(x,z)|^2$, in arbitrary units, during propagation for the waveguide structure of Fig. 4.

slow dependence of A on z. A rigorous proof of this statement can be obtained by application of the Floquet theory to Eq. (7) (see, e.g., Ref. [29]) or by a multiple-scale asymptotic analysis . For the sake of completeness, a brief explanation thereof, based on an asymptotic analysis of Eq. (7), is given in the Appendix, where the solution to Eq. (7) is written as an asympotic expansion, $\psi = \psi^{(0)} + \epsilon \psi^{(1)} + \epsilon^2 \psi^{(2)} + \cdots$. As a smallness parameter ϵ, we assumed the ratio between the modulation period Λ of axis distortion and the diffraction length of the fundamental mode for the straight waveguide [see Eq. (A3)]. At leading order in the expansion, it turns out that $\psi^{(0)}$ satisfies the averaged equation

$$\frac{\partial \psi^{(0)}}{\partial z} = \frac{i}{2k_0 n_0} \frac{\partial^2 \psi^{(0)}}{\partial x^2} + ik_0[n_{av}(x) - n_0]\psi^{(0)} + \cdots,$$

(10)

where the ellipses indicate terms of higher order than $\sim \epsilon$. The behavior found in the numerical simulations can easily be explained in term of the averaged equation (10). In fact, for the truncated parabolic-index profile [Eq. (8)], the average refractive index, given by Eq. (9), can be analytically computed after some straightforward, though tedious, algebra, yielding

$$n_{av}(x) = \begin{cases} n_0 + \dfrac{\Delta n_0}{\pi} \left\{ \dfrac{2a^2 - 2x^2 - A^2}{2a^2} \left[\arcsin\left(\dfrac{|x|+a}{A}\right) - \arcsin\left(\dfrac{|x|-a}{A}\right) \right] \right. \\ \qquad \left. + \dfrac{A}{2a} \left[\left(1 - \dfrac{3|x|}{a}\right) \sqrt{1 - \left(\dfrac{|x|+a}{A}\right)^2} + \left(1 + \dfrac{3|x|}{a}\right) \sqrt{1 - \left(\dfrac{|x|-a}{A}\right)^2} \right] \right\}, & |x| < A - a \\[2ex] n_0 + \dfrac{\Delta n_0}{\pi} \left\{ \dfrac{2a^2 - 2x^2 - A^2}{2a^2} \left[\dfrac{\pi}{2} - \arcsin\left(\dfrac{|x|-a}{A}\right) \right] \right. \\ \qquad \left. + \dfrac{A}{2a} \left(1 + \dfrac{3|x|}{a}\right) \sqrt{1 - \left(\dfrac{|x|-a}{A}\right)^2} \right\}, & A - a < |x| < A + a \\[2ex] n_0, & |x| > A + a \end{cases}$$

(11)

for $A > a$, and

$$n_{av}(x) = \begin{cases} n_0 + \Delta n_0 \dfrac{2a^2 - 2x^2 - A^2}{2a^2}, & |x| < a - A \\[2ex] n_0 + \dfrac{\Delta n_0}{\pi} \left\{ \dfrac{2a^2 - 2x^2 - A^2}{2a^2} \left[\dfrac{\pi}{2} - \arcsin\left(\dfrac{|x|-a}{A}\right) \right] \right. \\ \qquad \left. + \dfrac{A}{2a} \left(1 + \dfrac{3|x|}{a}\right) \sqrt{1 - \left(\dfrac{|x|-a}{A}\right)^2} \right\}, & a - A < |x| < a + A \\[2ex] n_0, & |x| > A + a \end{cases}$$

(12)

for $A < a$. A plot of $n_{av}(x)$, shown in Fig. 6, shows that, as the modulation depth A is increased to make it comparable and far larger than the waveguide size a, a strong reshaping of the average refractive index is observed, with the appearance of two peaks symmetrically placed away from $x = 0$. In such a regime, the "averaged waveguide" seen by the beam is equivalent to two straight waveguides which are weakly coupled to each other, and thus the beam splitting observed in Fig. 5 after the adiabatic section corresponds to light propagation along both of the two channels of the averaged waveguide. The effect of the adiabatic waveguide section in Figs. 4 and 5 is to slowly increase the modulation depth from zero to the final value A_0, i.e., to slowly modify the average refractive index profile, providing an adiabatic Y branch. We note that the two lowest-order eigenmodes of the averaged

waveguide correspond to the symmetric and antisymmetric supermodes usually encountered in the theory of coupled waveguides (see, for instance, Ref. [41]), so that the typical phenomenon of mode coupling between two waveguide channels, corresponding to dynamic tunneling in the quantum-mechanical analog problem, should be observable. We checked the occurrence of mode coupling by considering a uniformly modulated waveguide, i.e., with $A = A_0$ constant, with the injection of an *off-axis* Gaussian-like beam. As the offset of the injected field is chosen close to one of the two channels of the averaged waveguide, in fact, the mode coupling between the two channels of the waveguide is observed, as shown in Fig. 7. The periodic exchange of power between guided modes of the two adjacent waveguides in the average waveguide model is clearly evident from the figure.
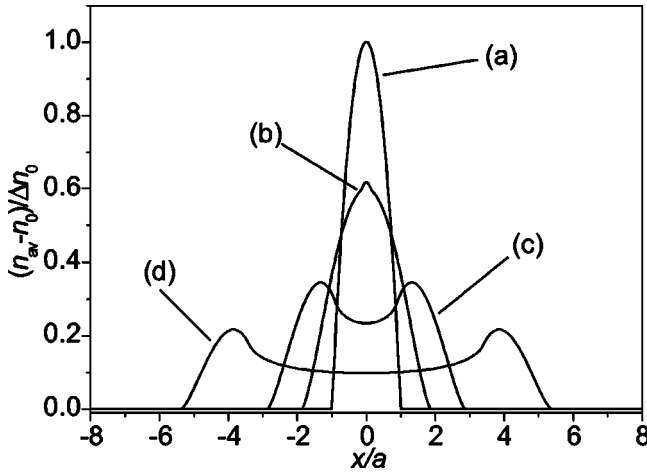
FIG. 6. Normalized average refractive index profile (n_{av} $-n_0)/\Delta n_0$ for the periodically-modulated parabolic truncated waveguide for a few values of the ratio A/a. Curve (a) $A/a=0$, curve (b) $A/a=7/8$, curve (c) $A/a=15/8$, curve (d) $A/a=4.375$.

B. Radiation-loss reduction

A phenomenon closely related to the wave packet dichotomy of a bound electron in an atom subjected to a high-frequency and superstrong laser field is the suppression of the ionization rate and the adiabatic stabilization of the wave function [26,32]. In fact, an atom in a strong laser field, of the order of the atomic unit, reacts to the increase in intensity or decrease in frequency by increasing its lifetime, i.e., its decay by multiphoton ionization can be quenched. The analogous optical counterpart in our waveguide model is the quenching of radiation loss associated to the beam splitting as the modulation depth of axis bending is increased. This result is rather exotic and not predictable when the weak axis bent limit, usually adopted to determine radiation losses in periodically bent waveguides, is adopted [40]. In the weak
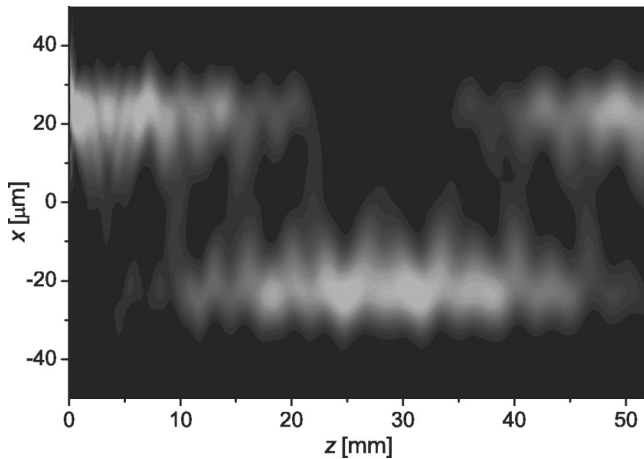

FIG. 7. Beam propagation and directional coupling in a uniformly modulated truncated parabolic waveguide with an off-axis Gaussian-like excitation at the input. The waveguide structure is the same as in Fig. 4, except than for the absence of the adiabatic zone, and $A/a=3.5$. The off-axis Gaussian-like excitation beam is centered at $x=A$ and has a waist of $\simeq 10~\mu$m.

bending limit, for which $A\ll a$, one can write $n[x-x_0(z)]$ $\simeq n(x)-(dn/dx)x_0(z)$, so that Eq. (7) takes the form

$$\frac{\partial\psi}{\partial z}=\mathcal{H}\psi+\mathcal{H}'\,\psi, \tag{13}$$

where the operators $\mathcal{H}$ and $\mathcal{H}'$ are given by

$$\mathcal{H}\equiv\frac{i}{2k_0n_0}\frac{\partial^2}{\partial x^2}+ik_0[n(x)-n_0],\quad \mathcal{H}'\equiv-ik_0\frac{dn}{dx}x_0(z). \tag{14}$$

By treating $\mathcal{H}'$ as a perturbation term, its effect is that of coupling the modes of the straight waveguide during the propagation. The radiation-loss rate for the fundamental eigenmode of the straight waveguide can be calculated by evaluating the coupling, induced by $\mathcal{H}'$, to the unbounded (continuous) modes of the waveguide using the Fermi golden rule. The result for the power loss rate 2α, when approximating the fundamental eigenmode with the Gaussian beam of the untruncated parabolic waveguide and the continuous modes as plane waves, has been analytically derived by Marcuse and reads [40]

$$2\alpha=\sqrt{\frac{4\pi}{k_0n_0}\left(\frac{2\pi}{\Lambda}-\beta_0\right)}\frac{A^2}{w_0^3}\exp\left[-k_0n_0w_0^2\left(\frac{2\pi}{\Lambda}-\beta_0\right)\right], \tag{15}$$

where $\beta_0=k_0\Delta n_0-(1/a)[\Delta n_0/(2n_0)]^{1/2}$ is the propagation constant of the fundamental Gaussian eigenmode of the straight waveguide and w_0 its size, given by

$$w_0=\sqrt{\frac{a}{k_0}\left(\frac{2}{n_0\Delta n_0}\right)^{1/2}}. \tag{16}$$

Equation (15) clearly shows that the loss rate increases as the amplitude A of modulation is increased. However, when the modulation period Λ is short enough and the modulation depth A becomes comparable or larger than the waveguide size a, the perturbative calculation leading to Eq. (15) fails, and a description based on the averaged beam propagation equation [Eq. (10)] is more suited to study the radiation-loss problem. We note that, at the leading order in the asymptotic analysis for which the averaged equation (10) is valid, there is a complete suppression of radiation losses after the adiabatic transition, since no coupling between the guided modes of the averaged (double-channel) waveguide and the radiation modes occurs. In this case, the existence of radiation losses comes out when higher-order terms are accounted for in the averaged equation, using either the multiple-scale asymptotic approach or the Floquet theory; a perturbative calculation in this case is much more involved and requires in any case numerical analysis (see, for instance, Ref. [32]). Following Refs. [33,42], a simpler approach to investigate the confinement properties of the modulated waveguide is based on a direct numerical integration of Eq. (7) on a finite transverse domain with absorbing boundary conditions, so that the radiation escaping from the integration window is lost during the propagation. The comparison of power levels
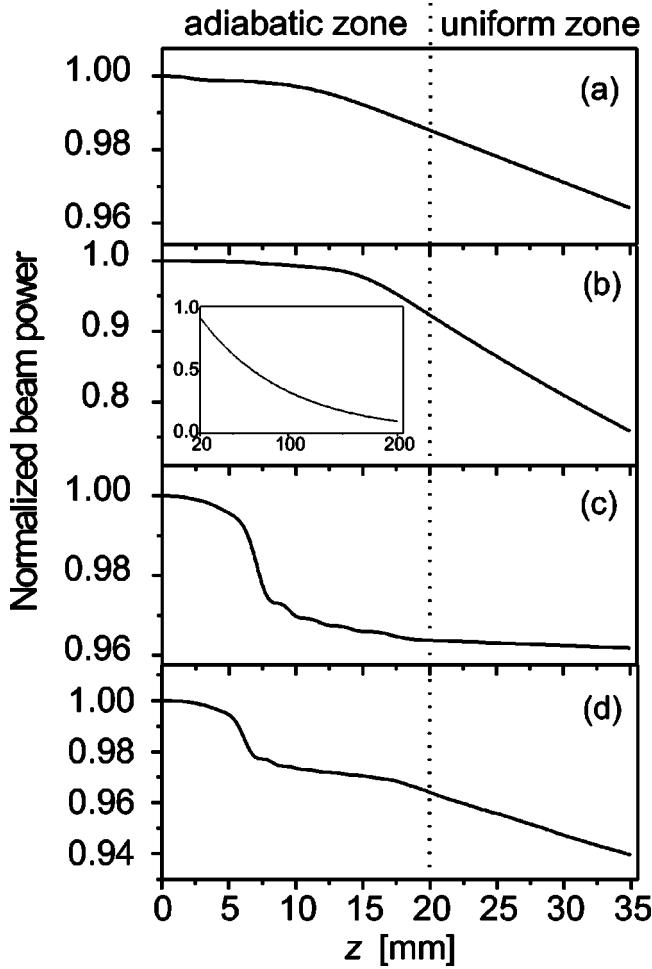
FIG. 8. Total beam power $P(z)$ versus propagation distance z in the waveguide structure of Fig. 4, as obtained by numerical integration of Eq. (7) with absorbing boundary conditions, for a few values of the ratio A_0/a: (a) $A_0/a=0.25$; (b) $A_0/a=0.75$; (c) $A_0/a=3.375$; (d) $A_0/a=4.375$. The integration window in the transverse x direction has a full width of 160 μm; the other parameter values are the same as in Fig. 4. The inset in Fig. 8(b) shows, as an example, the exponential decay law of beam power at longer propagation distances.

transmitted after propagation through waveguides with a fixed length but different modulation depths will provide an estimate of the radiation losses experienced by the field. As an example, in Fig. 8, we show the total beam power versus propagation distance, $P(z)=\int dx|\psi(z,x)|^2$, for increasing values of the ratio A/a. The waveguide geometry has been taken as in Figs. 4 and 5, and we assumed $P(0)=1$. Note that, in the uniform zone, the total beam power decreases with distance nearly exponentially [see, e.g., the inset in Fig. 8(b)], however the rate of attenuation is surprisingly *lower* in case of Fig. 8(c) ($A_0/a\simeq3.375$) and Fig. 8(d) ($A_0/a\simeq4.375$), than in case of Fig. 8(b) ($A_0/a\simeq0.75$). Figure 9 shows the numerically computed transmitted power $P(L)$ through a $L=35$-mm-long waveguide, normalized to the power level $P(L_a)$ on the plane $z=L_a=20$ mm at the end of the adiabatic section of the waveguide, versus the ratio A_0/a. As A_0/a is increased from zero, the power transmitted

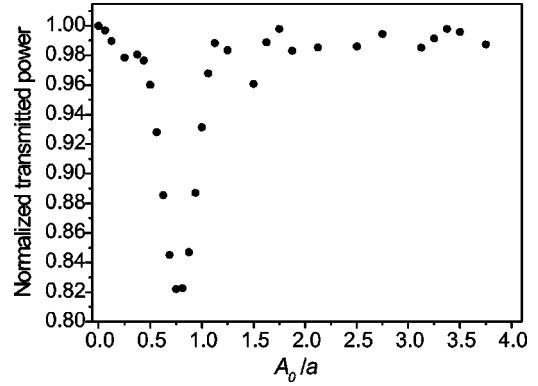FIG. 9. Normalized transmitted beam power $P(L)/P(L_a)$ in a $L=35$-mm-long waveguide, comprising a $L_a=20$-mm-long adiabatic region, versus normalized modulation depth A_0/a.

first decreases, until $A_0/a\simeq0.8$; a further increase of A_0/a leads to higher transmitted power and to the appearance of a double-peaked structure in the average refractive index profile (see Fig. 6).

IV. CONCLUSIONS

In this work, we have theoretically studied the properties of beam propagation in a periodically curved optical waveguide beyond the usual perturbative approach [40] and we have shown the occurrence of unusual effects, such as dynamic beam splitting and reduction of radiation losses. Such effects bear a close connection to similar phenomena encountered in the dynamics of a bound electron in an atom subjected to a superintense and high-frequency laser field. The analogy stems from the formal equivalence of the beam propagation problem in the scalar and paraxial wave approximations and the electronic wave function dynamics analyzed in the Kramers-Henneberger reference frame. Though our analysis has been focused on the simplest one-dimensional and scalar beam propagation equation, the physical picture underlying dynamic beam splitting and based on the average waveguide model discussed in Sec. III makes our results suitable for a generalization in more complex waveguide geometries. We envisage that our optical analogy may represent an experimentally accessible framework to study in the optical context many phenomena encountered in atomic physics with ultrahigh-intensity lasers, where their observation may be much more involved.

APPENDIX: DERIVATION OF THE AVERAGE WAVE EQUATION

In this appendix, we derive the averaged equation (10) describing, at leading order, the beam propagation in a periodically curved waveguide in the limit of a short modulation period Λ. To this aim, let us indicate by w_0 the typical size of the fundamental Gaussian-like mode of the straight waveguide with a truncated parabolic profile, as given by Eq. (8), and let us introduce the normalized spatial variables

$$\xi=\frac{z}{\Lambda}, \quad u=\frac{x}{a}. \tag{A1}$$

Using the scaled spatial variables given by Eq. (A1), the beam propagation equation (7) takes the form

$$\frac{\partial \psi}{\partial \xi} = i\epsilon \frac{\partial^2 \psi}{\partial u^2} + i\epsilon q(u,\xi)\psi, \tag{A2}$$

where we have set

$$\epsilon \equiv \frac{\Lambda}{2k_0 n_0 a^2}, \tag{A3}$$

and

$$q(u,\xi) = \begin{cases} 0 & \text{for} \quad |u| > 1 \\ k_0 2 k_0^2 a^2 n_0 \Delta n_0 \left\{ 1 - \left[u - \frac{A}{a} \cos(2\pi\xi) \right]^2 \right\} & \text{for} \quad |u| < 1. \end{cases} \tag{A4}$$

Note that, from a physical viewpoint, the dimensionless parameter ϵ represent basically the ratio between the modulation period of the axis bending and the diffractive length of the waveguide mode. To perform an asymptotic analysis of Eq. (A2), let us assume $\epsilon \ll 1$, and that the following scaling is satisfied: $k_0 a \sim \epsilon^{-1}$ and $\Delta n_0 \sim \epsilon^2$. Such a scaling ensures that the guiding term in Eq. (A2) is of the same order of magnitude, i.e., of order $\sim \epsilon$, than the diffractive term. We then search for a solution to Eq. (A2) as an asymptotic expansion:

$$\psi = \psi^{(0)} + \epsilon \psi^{(1)} + \epsilon^2 \psi^{(2)} + \cdots, \tag{A5}$$

and introduce multiple scales for ξ: $\xi_0 = \xi$, $\xi_1 = \epsilon\xi$, $\xi_2 = \epsilon^2\xi, \ldots$, to avoid the occurrence of secular growing terms in the asymptotic expansion. In order to include adiabatic changes of the axis modulation, we allow for the modulation depth A to vary on the spatial scale ξ_1. In this way, in Eq. (A4), one has $q = q(u;\xi_0,\xi_1)$. After setting expansion (A5) into Eq. (A2), using the derivative rule $\partial/\partial\xi = \partial/\partial\xi_0 + \epsilon\partial/\partial\xi_1 + \cdots$, a hierarchy of equations at successive corrections to ψ is obtained. At leading order, $\sim \epsilon^0$, one finds $\partial\psi^{(0)}/\partial\xi_0 = 0$, i.e., $\psi^{(0)} = \psi^{(0)}(u;\xi_1,\xi_2,\cdots)$ is independent of ξ_0. At order $\sim \epsilon$ one has

$$\frac{\partial \psi^{(1)}}{\partial \xi_0} = -\frac{\partial \psi^{(0)}}{\partial \xi_1} + i\frac{\partial^2 \psi^{(0)}}{\partial u^2} + iq(u;\xi_0,\xi_1)\psi^{(0)}. \tag{A6}$$

Since the right-hand side in Eq. (A6) is a periodic function with respect to ξ_0 with a period equal to one, in order to avoid the occurrence of secular growing terms when integrating Eq. (A6), we require

$$\int_0^1 d\xi_0 \left[-\frac{\partial \psi^{(0)}}{\partial \xi_1} + i\frac{\partial^2 \psi^{(0)}}{\partial u^2} + iq(u;\xi_0,\xi_1)\psi^{(0)} \right] = 0, \tag{A7}$$

which yields

$$\frac{\partial \psi^{(0)}}{\partial \xi_1} = i\frac{\partial^2 \psi^{(0)}}{\partial u^2} + i\left[\int_0^1 q(u;\xi_0,\xi_1)d\xi_0 \right]\psi^{(0)}. \tag{A8}$$

Note that the fast modulation of the waveguide axis curvature produces a fast change (i.e., on the scale ξ_0) of the beam envelope ψ at the order $\sim \epsilon$, which is obtained after integration of Eq. (A6). If we stop the asymptotic analysis to this order, the evolution equation for $\psi^{(0)}$ reads $\partial\psi^{(0)}/\partial\xi = \epsilon\partial\psi^{(0)}/\partial\xi_1$; using Eq. (A8) and reintroducing the original unscaled variables [see Eq. (A1)], one finally obtains

$$\frac{\partial \psi^{(0)}}{\partial z} = \frac{i}{2k_0 n_0}\frac{\partial^2 \psi^{(0)}}{\partial x^2} + ik_0[n_{av}(x,z) - n_0]\psi^{(0)}, \tag{A9}$$

where $n_{av}(x,z) = (1/\Lambda)\int_0^\Lambda dz\, n[x - A\cos(2\pi z/\Lambda)]$ is the averaged refractive index profile of the waveguide. The dependence of n_{av} on z comes from the possible slow dependence of the modulation depth A on z. By pushing the asymptotic analysis to the order $\sim \epsilon^3$, higher-order terms would appear in Eq. (A9), which are responsible for radiation losses for the average waveguide structure even in absence of the slow variations of modulation depth A.

[1] J. Evans, Am. J. Phys. **61**, 347 (1993).

[2] C. Tzanakis, Eur. J. Phys. **19**, 69 (1998).

[3] A.M. Steinberg, P.G. Kwiat, and R.Y. Chiao, Phys. Rev. Lett. **71**, 708 (1993).

[4] Ch. Spielmann, R. Szipöcs, A. Stingl, and F. Krausz, Phys. Rev. Lett. **73**, 2308 (1994).

[5] P. Balcou and L. Dutriaux, Phys. Rev. Lett. **78**, 851 (1997).

[6] L. Sirko, P.M. Koch, and R. Blumel, Phys. Rev. Lett. **78**, 2940 (1997).

[7] R. Morandotti, U. Peschel, J.S. Aitchison, H.S. Eisenberg, and Y. Silberberg, Phys. Rev. Lett. **83**, 4756 (1999).

[8] T. Pertsch, P. Dannberg, W. Elflein, A. Brauer, and F. Lederer,

Phys. Rev. Lett. **83**, 4752 (1999).

[9] G. Lenz, I. Talanina, and C.M. de Sterke, Phys. Rev. Lett. **83**, 963 (1999).

[10] M. Feldmann, J. Opt. Soc. Am. **61**, 446 (1971).

[11] G. Eichmann, J. Opt. Soc. Am. **61**, 161 (1971).

[12] E.E. Bergmann, Appl. Opt. **11**, 113 (1972).

[13] J.A. Arnaud, J. Opt. Soc. Am. **65**, 174 (1975).

[14] T.C. Guo and W.W. Guo, J. Appl. Phys. **52**, 635 (1981).

[15] W.K. Kahn and S. Yang, J. Opt. Soc. Am. **73**, 684 (1983).

[16] R. Castillo, A.K. Ghatak, and H. Hora, Appl. Sci. Res. **41**, 359 (1984).

[17] R.J. Black and A. Ankiewicz, Am. J. Phys. **53**, 554 (1985).

[18] A.K. Ghatak and E. Sauter, Eur. J. Phys. **10**, 136 (1989).

[19] E. Sauter and A.K. Ghatak, Eur. J. Phys. **10**, 144 (1989).

[20] N. Marinescu, Prog. Quantum Electron. **16**, 183 (1992).

[21] R.A. Abram, Opt. Commun. **12**, 338 (1974).

[22] J. D. Joannopoulos, R. D. Meade, and J. N. Winn, *Photonic Crystals* (Princeton University, Princeton, NJ, 1995).

[23] K. Sakoda, *Optical Properties of Photonic Crystals* (Springer-Verlag, Berlin, 2001).

[24] H. A. Kramers, *Collected Scientific Papers* (North-Holland, Amsterdam, 1956), p. 866.

[25] W.C. Henneberger, Phys. Rev. Lett. **21**, 838 (1968).

[26] M. Protopapas, C.H. Keitel, and P.L. Knight, Rep. Prog. Phys. **60**, 389 (1997).

[27] M. Gavrila, *Atoms in Intense Laser Fields* (Academic, Boston, 1992), p. 3.

[28] M. Gavrila and J.Z. Kamiński, Phys. Rev. Lett. **52**, 613 (1984).

[29] M. Pont, N.R. Walet, M. Gavrila, and C.W. McCurdy, Phys. Rev. Lett. **61**, 939 (1988).

[30] Q. Su, J.H. Eberly, and J. Javanainen, Phys. Rev. Lett. **64**, 862 (1990).

[31] M. Dörr, R.M. Potvliege, D. Proulx, and R. Shakeshaft, Phys. Rev. A **43**, 3729 (1991).

[32] R.J. Vos and M. Gavrila, Phys. Rev. Lett. **68**, 170 (1992).

[33] R. Dum, A. Sanpera, K.-A. Suominen, M. Brewczyk, M. Kus, K. Rzazewski, and M. Lewenstein, Phys. Rev. Lett. **80**, 3899 (1998).

[34] J. A. Arnaud, *Beam and Fiber Optics* (Academic, New York, 1976), pp. 173–177.

[35] M. J. Adams, *An Introduction to Optical Waveguides* (Wiley, New York, 1981).

[36] R. Accornero, M. Artiglia, G. Coppa, P. di Vita, G. Lapenta, M. Potenza, and P. Ravetto, Electron. Lett. **26**, 1959 (1990).

[37] T. Suhara, Y. Handa, H. Nishihara, and J. Koyama, J. Opt. Soc. Am. **69**, 807 (1979).

[38] R. Akridge, Am. J. Phys. **63**, 141 (1995).

[39] A. Hardy, Appl. Phys. B **18**, 223 (1979).

[40] D. Marcuse, Appl. Opt. **17**, 755 (1978).

[41] A. Yariv, *Quantum Electronics*, 2nd ed. (Wiley, New York, 1989), p. 631.

[42] J. Saijonmaa and D. Yevick, J. Opt. Soc. Am. **73**, 1785 (1983).